Determination of the von Klitzing constant and the fine-structure constant through a comparison of the quantized Hall resistance and the ohm derived from the NIST calculable capacitor

A. Jeffery, R. E. Elmquist, J. Q. Shields, L. H. Lee, M. E. Cage, S. H. Shields and R. F. Dziuba

Abstract. This paper describes a recent determination of the von Klitzing constant and the fine-structure constant by comparisons of values of the ohm as defined in the International System of Units (SI), derived from the National Institute of Standards and Technology (NIST) calculable cross-capacitor, and values of the international practical unit of resistance derived from the integral quantum Hall effect. In this determination, the comparisons were made in a series of measurements lasting three years. A small difference is observed between this determination and an earlier comparison carried out in this laboratory and reported in 1988. The most recent value of the fine-structure constant based on the experimental value and theoretical expression for the magnetic moment anomaly of the electron, which has the smallest uncertainty of any value currently available, is consistent with both of these results. The new value exceeds the 1990 conventional value of the von Klitzing constant $R_{K\text{-}90}$ by slightly more than twice the relative standard uncertainty of the present measurement, which is 2.4×10^{-8}.

1. Introduction

1.1 The calculable capacitor and realizations of the ohm at the NIST

Thompson and Lampard showed in 1956 [1] that the relation of the cross-capacitances of a cylindrical cross-capacitor is given by

$$\exp(-\pi C_1/\varepsilon_0) + \exp(-\pi C_2/\varepsilon_0) = 1, \qquad (1)$$

where C_1 and C_2 are the cross-capacitances per unit length between pairs of opposite electrodes and ε_0 is the electric constant (permittivity of vacuum). The value of this specially designed cross-capacitor can then be determined from a single length measurement. In the 1960s, calculable cross-capacitors built on this principle were first used to link capacitance and resistance to the SI units of length and time. The first report of a measurement based on a calculable cross-capacitor at the National Institute of Standards and Technology (NIST), then the National Bureau of Standards (NBS), was in 1961 by Cutkosky [2]. Cutkosky obtained the value of the US Legal Ohm based on standard resistors with a relative standard uncertainty of 2.1 μΩ/Ω using horizontally mounted cylindrical gauge bars as capacitor electrodes. Around the same time, Clothier [3] constructed a calculable capacitor that was used, starting in 1963, in Australian comparisons to realize the SI farad and SI ohm with a relative standard uncertainty of less than 1×10^{-7}.

A new cross-capacitor was constructed at the NIST in the late 1960s which utilized the geometry of Clothier, and this capacitor is still the one used today. In 1974 Cutkosky [4] reported an assignment of an SI value to the US Legal Farad and the US Legal Ohm, then maintained as a bank of 10 pF fused-silica capacitors [5] and a bank of 1 Ω Thomas-type resistors, respectively. The realization of the ohm in terms of the SI units of length and time was assigned a relative standard uncertainty of 0.03 μΩ/Ω. Shields et al. [6] reported the second NBS realization of the ohm and farad in 1989 using the same system after making several improvements. The reported relative uncertainties were 0.022 μΩ/Ω for the US Legal Ohm and 0.014 μF/F for the US

A. Jeffery, R. E. Elmquist, J. Q. Shields, L. H. Lee, M. E. Cage, S. H. Shields and R. F. Dziuba: National Institute of Standards and Technology, Gaithersburg, MD 20899-0001, USA.*

* Electricity Division, Electronic and Electrical Engineering Laboratory, Technology Administration, US Department of Commerce. Official contribution of the National Institute of Standards and Technology, not subject to copyright in the United States.

Legal Farad. These uncertainties represent standard uncertainties (i.e. one standard deviation estimates) which are used throughout this paper. The measurement process from the calculable capacitor through the fused-silica capacitors to the unit of resistance maintained at the NIST, now based on the quantum Hall effect (QHE), is known collectively as the calculable capacitor chain (Figure 1); this is described in detail.

1.2 The von Klitzing constant

The four-terminal quantized Hall resistance (QHR) of the i-th integer QHE plateau is $R_{\mathrm{H}}(i) = R_{\mathrm{K}}/i$, where R_{K} is the von Klitzing constant. It is generally accepted that R_{K} is related to the fine-structure constant α by

$$R_{\mathrm{K}} = h/e^2 = (\mu_0 c)/(2\alpha), \tag{2}$$

where h is the Planck constant and e is the elementary charge. The magnetic constant (permeability of vacuum), $\mu_0 = 4\pi \times 10^{-7}$ N/A^2, and the speed of light in vacuum, $c = 299\,792\,458$ m/s, are exactly defined in the SI. The validity of (2) is supported by arguments based on gauge invariance [7] for an ideal quantized two-dimensional electron gas (2-DEG). Further studies have shown how dissipationless QHE behaviour can be maintained in finite, disordered 2-DEG systems [8, 9] and at substantial current density [10, 11].

Recently, the ohm derived from the calculable capacitor has been combined with QHE measurements to provide some of the best determinations, expressed in terms of SI units, of the von Klitzing constant [12] and the fine-structure constant. One of these SI determinations was the NIST value of the von Klitzing constant derived from the calculable capacitor reported in 1989. This value is 25 812.807 23(61) Ω [13], and represents measurements for a mean date of 17 May 1988. The best value of R_{K} and other fundamental constants are calculated through a least-squares analysis procedure [14, 15]. By international agreement, the 1990 conventional value of R_{K} is

$$R_{\mathrm{K-90}} = 25\,812.807\ \Omega.$$

This value is exact, but in terms of the expected agreement with the SI value of R_{K}, the $R_{\mathrm{K-90}}$ value has been assigned a relative standard uncertainty of 2×10^{-7}, or 0.005 Ω [16], using all available experimental data.

In 1993, the NIST began a new determination of the von Klitzing constant derived from the calculable capacitor. A small difference between the initial results for this new comparison and the 1988 result led to a detailed investigation of our measurement systems. While the difference was smaller than the assigned uncertainty to the 1990 conventional value of the von Klitzing constant, it is larger than our experimental uncertainty for this measurement. In 1996, the result for this new comparison was reported in [17]. This paper describes in detail the extensive investigations performed to try to account for this difference and gives the final result.

2. Calculable capacitor experiment

The present geometry of the calculable capacitor at the NIST [4] consists of vertical cylindrical bars arranged at the corners of a square in the x-y plane. Capacitance is measured between diagonal pairs of opposite bars, which for this geometry gives two capacitances $C_1 \approx C_2$. The Thompson-Lampard equation (1) reduces to $C \approx 2$ pF/m, where $C = (C_1 + C_2)/2$. Second-order terms due to the difference between C_1 and C_2 contribute less than $10^{-9}\ C$ to this capacitance in the NIST calculable capacitor.

The calculable capacitor at the NIST comprises four 6.35 cm diameter bars with clearances of 3.60 mm between adjacent bars. A cylindrical electrode is partially inserted on the central z axis, midway between the four bars, such that a change in the vertical position of the electrode effectively changes the length of the two cross-capacitances C_1 and C_2. This movable blocking electrode with a diameter of 2.72 cm is positioned by polytetrafluoroethylene (PTFE) rings. The other end of the cross-capacitor is defined by a similar fixed blocking electrode. Measurements are made by comparing a fixed-value capacitor with the calculable capacitor at two positions of the movable electrode. The length measurement is then the displacement of the electrode between these two positions. The displacement is found using a Fabry-Pérot interferometer which measures the relative displacement of optical flats mounted in the movable and fixed blocking electrodes. From this length measurement and (1) the value of the calculable capacitor is determined and a value is assigned to the fixed capacitor.

3. AC measurements

The NIST calculable capacitor chain is a sequence of measurements which realizes an SI value of the US representation of the ohm and of the farad and, since 1988, an SI value of the von Klitzing constant R_{K}. This sequence is shown in Figure 1. The bridge measurements which make up the ac part of the chain are essentially the same as reported in 1974 and 1989 [4, 6]. The artefact standards used in the chain, except the calculable capacitor, all drift in value over time. Groups of measurements in the calculable capacitor chain are performed in a particular sequence so that averaging helps to eliminate the effect of the linear drift. This sequence is shown in Figure 2.

The measurement sequence for the ac part of the chain involves seven main bridge measurements. Most of the bridges in the chain are four-terminal-pair so that the standards used in these bridges meet certain

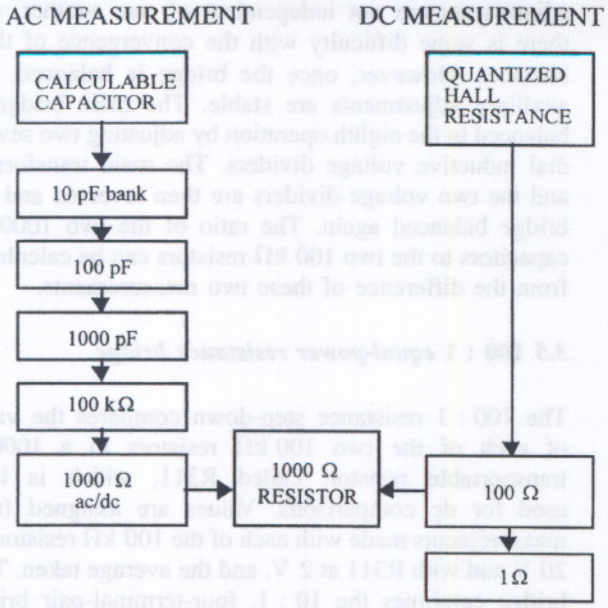

Figure 1. Basic measurement steps of the NIST calculable capacitor chain.

defining conditions at each terminal-pair [18]. This creates well-defined standards which can be moved between different bridges and still provide the same value. All the ac measurements are made at a frequency of 1592 Hz. The following paragraphs describe the ac bridge measurements and accompanying auxiliary measurements used to determine certain parameters.

3.1 Calculable capacitor measurement

As noted above, the first step (labelled 1 in Figure 2) is the comparison of the calculable capacitor to a fixed 10 pF standard. The 10 pF transportable fused-silica reference capacitor is actually compared with the calculable capacitor configured at two different values, 0.2 pF and 0.7 pF, and the difference between the two measurements is used to assign a value to the 10 pF standard. The bridge used in this comparison has a special transformer which supplies 200 V at 1592 Hz to the cross-capacitor. The reference capacitor is connected to a tap that supplies 4 V for the 0.2 pF comparison or to a second tap that supplies 14 V for the 0.7 pF comparison. The bridge is balanced by injecting the necessary current at the detector through a second 10 pF capacitor and an adjustable voltage divider. Quadrature adjustment is provided by injection through a suitable conductance and another voltage

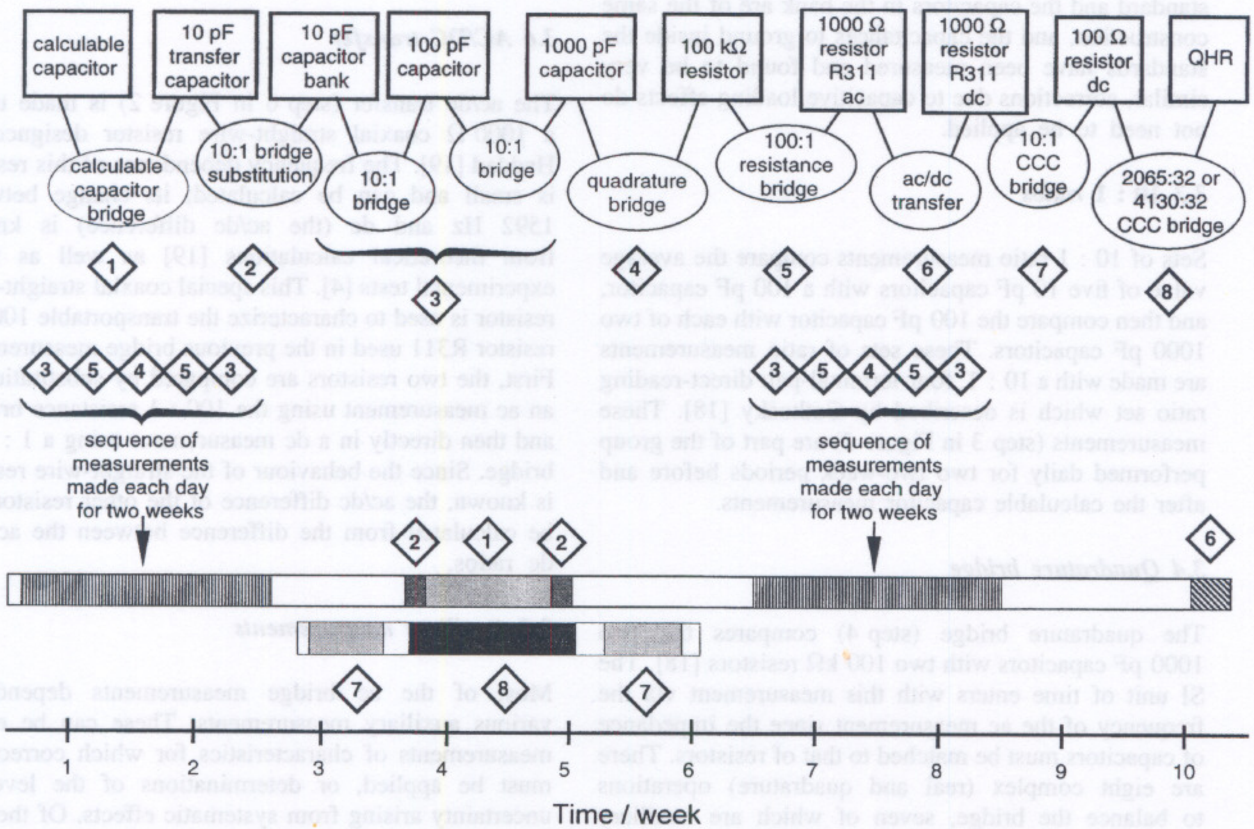

Figure 2. Standards, bridge measurements, and sequence of measurement steps used in the NIST calculable capacitor chain. The bridge measurements, labelled 1 through 8, are performed in a time sequence to reduce uncertainty from drift and failure to close. Following the pattern shown, the main measurements can be completed in approximately ten weeks. Auxiliary measurements, which are not shown, can take many months.

divider. The bridge is two-terminal-pair, so auxiliary measurements are necessary to account for the effects of capacitances and inductances in the cables and the calculable capacitor bars.

3.2 Transfer to the 10 pF bank

After the 10 pF transportable fused-silica capacitor is measured against the calculable capacitor, it is moved to the capacitance standards laboratory where it is measured against a bank of five 10 pF fused-silica standards [5] (step 2 in Figure 2). These standards, which were designed and fabricated at the NIST, are maintained in an oil bath at 25 °C. They have an average drift rate of 10 nF/F per year, which allows them to be used to maintain the NIST realization of the farad for several months between calculable capacitor measurements. The comparison between the transportable standard and the bank provides a correction, which is used to convert results of measurements made with the bank to values which are in agreement with the SI unit obtained from the calculable capacitor. All comparisons are made by the sequential substitution of each of the 10 pF fused-silica standards. The transfer measurements are made with a two-terminal-pair 10 : 1 transformer bridge using a 100 pF capacitor as a fixed reference. Since the transfer standard and the capacitors in the bank are of the same construction, and the capacitances to ground inside the standards have been measured and found to be very similar, corrections due to capacitive loading effects do not need to be applied.

3.3 10 : 1 ratios

Sets of 10 : 1 ratio measurements compare the average value of five 10 pF capacitors with a 100 pF capacitor, and then compare the 100 pF capacitor with each of two 1000 pF capacitors. These sets of ratio measurements are made with a 10 : 1, four-terminal-pair direct-reading ratio set which is described by Cutkosky [18]. These measurements (step 3 in Figure 2) are part of the group performed daily for two two-week periods before and after the calculable capacitor measurements.

3.4 Quadrature bridge

The quadrature bridge (step 4) compares the two 1000 pF capacitors with two 100 kΩ resistors [18]. The SI unit of time enters with this measurement via the frequency of the ac measurement since the impedance of capacitors must be matched to that of resistors. There are eight complex (real and quadrature) operations to balance the bridge, seven of which are auxiliary adjustments required to meet the defining conditions for a four-terminal-pair measurement. A combining network [18] is used to reduce the number of detectors required for these auxiliary balances. Certain auxiliary adjustments are not independent of one another, and there is some difficulty with the convergence of their balances. However, once the bridge is balanced, the auxiliary adjustments are stable. The main bridge is balanced in the eighth operation by adjusting two seven-dial inductive voltage dividers. The main transformer and the two voltage dividers are then reversed and the bridge balanced again. The ratio of the two 1000 pF capacitors to the two 100 kΩ resistors can be calculated from the difference of these two measurements.

3.5 100 : 1 equal-power resistance bridge

The 100 : 1 resistance step-down compares the value of each of the two 100 kΩ resistors to a 1000 Ω transportable resistor, called R311, which is later used for dc comparisons. Values are assigned from measurements made with each of the 100 kΩ resistors at 20 V and with R311 at 2 V, and the average taken. This bridge combines the 10 : 1, four-terminal-pair bridge used to determine the 10 : 1 ratios and a separate 10 : 1 current transformer in order to put equal power in the resistance standards and obtain good sensitivity while minimizing heating effects [18]. This step-down (step 5 in Figure 2) is done immediately before and after the quadrature bridge measurement and is part of the set of measurements made daily for two two-week periods.

3.6 AC/DC transfer

The ac/dc transfer (step 6 in Figure 2) is made using a 1000 Ω coaxial straight-wire resistor designed by Haddad [19]. The frequency dependence of this resistor is small and can be calculated; its change between 1592 Hz and dc (the ac/dc difference) is known from theoretical calculations [19] as well as from experimental tests [4]. This special coaxial straight-wire resistor is used to characterize the transportable 1000 Ω resistor R311 used in the previous bridge measurement. First, the two resistors are compared by substitution in an ac measurement using the 100 : 1 resistance bridge, and then directly in a dc measurement using a 1 : 1 dc bridge. Since the behaviour of the straight-wire resistor is known, the ac/dc difference of the other resistor can be calculated from the difference between the ac and dc ratios.

3.7 Auxiliary measurements

Most of the ac bridge measurements depend on various auxiliary measurements. These can be either measurements of characteristics for which corrections must be applied, or determinations of the level of uncertainty arising from systematic effects. Of the first type, some very stable characteristics only need to be checked every few years, while less stable ones must be determined every time the bridge measurement is made. A very thorough investigation of these auxiliary measurements was carried out to determine whether corrections, which in some cases had been assumed to be stable, had changed significantly in the time between the checks. The time when the auxiliary measurements are made is not shown in Figure 2. Some measurements are made at the same time as the corresponding measurement, while others are made in the months before and after the principal set of measurements shown in Figure 2.

3.7.1 Uncertainty due to geometric imperfections

Uncertainty due to geometric imperfections is one of the largest sources of uncertainty for the calculable capacitor experiment. This includes the relative alignment of the axes of the bars to each other and to the blocking electrode, alignment of the electrical axis of the capacitor and the optical axis of the interferometer, and imperfections in the bars. The primary way in which geometrical effects are evaluated is by measurements of the capacitances between insulated bands on the blocking electrode and each of the four bars. The distances between the two insulated bands used as probes and each of the bars can be calculated from these capacitance (probe) measurements. These probe measurements allow us to measure changes in the separation of the bars along the length of the calculable capacitor and changes in the excentricity of the blocking electrode. Two insulated bands are needed on the blocking electrode so that the tilt of the blocking electrode can also be calculated.

The alignment of the calculable capacitor electrodes with the Fabry-Pérot interferometer is also evaluated using these probe measurements. From the original interferometer alignment there are known probe capacitance values which correspond to the position where the electrical axis of the capacitor is perfectly aligned with the optical axis of the Fabry-Pérot interferometer. The probe measurements that correspond to this perfect alignment are obtained using an iterative process which is performed with the top enclosure of the calculable capacitor removed. The upper blocking electrode is positioned in the calculable capacitor so that the electrical and optical axes are closely aligned. The interferometer is then aligned by adjusting the tilt of the lower blocking electrode. The upper electrode is then rotated by 180° and the interferometer aligned without moving the lower blocking electrode. The probe measurements for the perfect alignment are found from the average of probe measurements made at the two positions of the upper blocking electrode. This procedure is then repeated, starting with the probe at the position obtained from the initial measurements, until the measurements corresponding to the perfect alignment are within the required uncertainty.

The tilt of the blocking electrode, which is known from the probe measurements, is related to the tilt of the optical axis since the upper optical flat is mounted in this electrode. By comparing these measurements with those corresponding to perfect alignment, the angle between the calculable capacitor axis and the optical axis of the interferometer can be found. This angle was 34 μrad, which corresponds to a relative correction of 6×10^{-10} to the value assigned to the 10 pF standard. The separations of the calculable capacitor electrodes were also measured; they have remained constant since 1988 to within 0.1 μm, which is the uncertainty of our measurement.

Recent linearity tests of the calculable capacitor were made by measuring 0.1 pF increments along the length of the capacitor. The differences between measurements were larger than the uncertainty assigned to this systematic effect in 1989 and 1974, and could not be accounted for by uniform changes in the separation of the electrodes. These differences are believed to be due to the effect of local imperfections and/or excentricity of the movable and fixed blocking electrodes. These effects would not be removed by the spike on the end of both the upper and lower blocking electrodes which is designed to reduce the effect of a uniform taper of the main electrodes. The earlier evaluation of uncertainty arising from non-linearity of the capacitor was made on the basis of experimental tests done by Clothier [3]. However, these recent linearity tests have led us to increase the relative standard uncertainty due to geometrical imperfections from 5×10^{-9}, which was assigned in 1974 [4], to 15×10^{-9}, the standard deviation of the 0.1 pF increment measurements.

3.7.2 Transformer ratios

Transformer ratios are generally stable, and for some NIST bridge transformers the ratios have changed by only 1×10^{-9} or 2×10^{-9} over twenty years. The transformer ratio of the calculable capacitor bridge is determined by using capacitors of known value in the same ratios used when comparing the calculable capacitor with the 10 pF capacitor. The transformer ratio for the calculable capacitor bridge was measured and found to have a relative difference of 5×10^{-9} from its previous value, as measured in 1987. This correction was applied in the new calculable capacitor measurements.

The bridge transformer 10 : 1 ratios are measured by the permutation of eleven 10 pF capacitors [20, 21]. This method ensures that the 10 : 1 ratios are obtained in a way strictly comparable with that used in the 10 : 1 step-ups from 10 pF to 100 pF and from 100 pF to 1000 pF. The relative difference between present and previous measurements of the four-terminal-pair 10 : 1 bridge transformer ratio was less than 1×10^{-9}.

The 100 : equal-power resistance bridge ratio is derived from a combination of the four-terminal-pair 10 : 1 bridge voltage transformer ratio and a 10 : 1 current transformer ratio. The current transformer is calibrated by reversing the way it is connected in the four-terminal-pair 10 : 1 bridge so that the combined bridge ratio is 1 : 1. By measuring the ratio of two 1000 pF capacitors with this 1 : 1 bridge and then measuring the ratio with the position of the two standards in the bridge reversed, the current transformer ratio can be found relative to that of the four-terminal-pair bridge 10 : 1 voltage transformer.

From the 1970s until 1994, the measurements of the 100 : 1 equal-power resistance bridge combined transformer ratio just described were made periodically and found to be stable within a few times 10^{-9} of the ratio. However, in June 1994, this transformer ratio was measured again and showed a relative difference of 3×10^{-8} from its previous value. This new ratio remained unchanged for a series of measurements from 6 June 1994 until 23 September 1994. The next measurement in December 1994 indicated that the ratio had returned to its original value. The transformer ratio was carefully monitored at the time of the December 1994 (SI) ohm determination. Further changes have not been observed since that time.

3.7.3 Bridge characteristics

The linearity of the real and quadrature bridge adjustments (dials) and the phase defect of a bridge are characteristics that are measured only periodically. Linearity is usually checked [18] by a build-up process based on repeatedly adding a stable admittance in parallel with one side of the bridge. The bridge reading is noted and the added admittance removed. A variable admittance in parallel on the other side of the bridge is adjusted to obtain the same bridge reading and the stable admittance added again. This step-by-step comparison of the dial readings ensures that the same admittance produces the same change at different ranges of the bridge dials. The linearity was satisfactory when the 10 : 1 four-terminal-pair bridge was originally constructed and was found to be stable over time. For the present work, a check of the linearity was made by comparisons against a new four-terminal-pair bridge that had recently been constructed at the NIST [22]. Since the two four-terminal-pair bridges agree for comparisons of various standards, it is assumed that the linearities of both bridges are adequate.

Phase defect is checked by making sure no change in the real dials is observed when a purely quadrature admittance is added in parallel with one of the admittances in the bridge. The phase defect of the four-terminal-pair bridge was checked by setting up the bridge with resistors and adding a 10 pF fused-silica capacitor that has a very small phase defect, thus assuring that the admittance added is purely quadrature. A quadrature bridge was used to determine the phase angles of the resistors used in the bridge. If the phase angles of the standards in the bridge are not known, erroneous results may be obtained with this method. The deviations from linearity and phase defects were found to be within the allotted uncertainties given in Tables 1 and 2. Comparisons with previous measurements [18] of the nonlinearities showed them to be relatively constant.

Further characterization of the bridge includes the determination of the magnitude of the real and quadrature dials by adding a known real component and a known quadrature component to the standards in the bridge. This changes the reading of the bridge dials and, since the added components are known, the actual change in the bridge reading can be compared with the expected change. A method to measure an admittance that is 1/1000 of the bridge standards is needed to calibrate the known real component since 1000×10^{-6} is the full scale on the bridge dials, while the quadrature component can be evaluated with a quadrature bridge. This evaluation was performed when the bridge was first built and again in the mid-1980s and found not to have changed. For this comparison, a check of the magnitude of the bridge adjustments was made through a comparison with the newly constructed four-terminal-pair bridge, for a 10 : 1 ratio of 1000 pF and 100 pF capacitance standards [22]. A 0.17 pF capacitor was added in parallel on the low-voltage side to create a significant change in the bridge reading, and both bridges were used to measure this difference. The relative agreement of the bridges was 3×10^{-9} for this setup, which was within the known stability of the 0.17 pF standard, indicating that the magnitude of the bridge adjustments was satisfactory.

The bridge adjustments that have been discussed to this point include only the 10 : 1 four-terminal-pair bridge, which uses specially designed inductive voltage dividers made at the NIST [18]. This bridge is part of the 100 : 1 resistance bridge, so the calibration of the bridge adjustments is the same. The dials for adjustment of the other bridges, specifically the calculable capacitor bridge and the quadrature bridge, use commercial inductive voltage dividers. The linearity and magnitude of the bridge dials being used in these bridges are thus based on the specifications of the dividers given by the manufacturer. These specifications have also been measured by NIST calibration laboratories, and are satisfactory for the amount of adjustment required by our bridges. The phase defect, however, is fairly large; the effect on the real dials is calculated and included in the uncertainty of the measurement.

3.7.4 Voltage dependence

Some variation of capacitance with applied voltage may be expected. The voltage dependence of capacitance standards are assessed using three $33\frac{1}{3}$ pF capacitors which are constructed so that they have very low voltage dependence [23]. These capacitors can be configured together in several ways. In parallel, the three standards form a single 100 pF capacitor, which can be used to determine the voltage dependence of 100 pF standards. Another method involves a comparison of a permutation of the three $33\frac{1}{3}$ pF standards in a 2 : 1 bridge with a permutation of three 10 pF standards in the same bridge. From this the average voltage dependence of the 10 pF capacitors can be found. A series of 1 : 1 comparisons between the three 10 pF capacitors yields the individual voltage dependences. The voltage dependence of three 1000 pF standards can be determined in the same way.

The voltage dependence of the 10 pF fused-silica capacitor at 4 V, 14 V, and 200 V must be known. It is measured close to the time the SI ohm determination is performed. In addition, the voltage dependence of the 100 pF capacitor between 20 V and 200 V must also be corrected since this standard is used at both voltages in the calculable capacitor chain. Voltage dependence of 1000 pF capacitors are needed for the 100 : 1 transformer ratio measurement where the capacitors are used at different voltages than those used in the calculable capacitor chain.

3.7.5 Coaxial chokes

Coaxial chokes [18, 24] were used in the bridges in every step of the SI ohm determination to reduce net currents in the coaxial cables used in the bridges. Negligible net current implies that the current in the shield is equal and opposite to the current in the inner conductor. Since the resulting magnetic field exterior to the cable is zero, this eliminates possible inductive couplings between cables and the bridge systems. Another aspect of using chokes is that, when used in combination with ground loops, they create a well-defined system by reducing the effect of stray magnetic fields on the bridge system. If a magnetic field induces an emf in the bridge system and no choke is present, large currents can flow and cause errors in the final balance point. If an emf is induced in the shield of a choked coaxial cable, most of the voltage drop is across the choke since it has a high impedance compared with the impedance of the shield itself. Since both the shield and the inner conductor of the cable are wound through the choke's core, the choke behaves like a 1 : 1 transformer and there is an equivalent voltage drop across the inner conductor, reducing the effect of the magnetic field.

The choke attenuates the net current by a factor of several hundred; therefore any current remaining is usually small. These choke corrections were evaluated for every choke in all of the bridges in the calculable capacitor chain. Choke corrections were also determined for bridges used to measure transformer ratios and voltage dependences. The sum of the relative choke corrections for any of the bridges was no greater than 2×10^{-9}.

3.7.6 Harmonics

The quadrature bridge matches the impedances of capacitors to resistors and therefore requires an accurate measurement of frequency. Special filters are used in the bridge to eliminate harmonics of the fundamental frequency and the associated uncertainty is evaluated. Measurements of the possible errors are made by amplifying the signal from each harmonic 100 times and measuring the effect on the bridge dials. In this way, the relative standard uncertainty due to harmonics in the quadrature bridge (1000 pF to 100 kΩ) was evaluated and found to be less than 1×10^{-9}.

4. DC measurements

Comparisons between the US representation of the ohm and the quantum Hall resistance (QHR) began on a regular basis in 1983. Beginning in 1986, an automated potentiometric measurement system [25] was used to produce very low relative uncertainty in comparisons between the 6453.2 Ω plateau in GaAs/GaAlAs heterostructure devices and several 6453.2 Ω transfer resistors. The transfer resistors were measured against Hamon devices [26], which were designed to satisfy the nominal ratio equations between series, series-parallel, and parallel configurations, to a relative uncertainty of less than 1×10^{-8}. Automated direct-current comparator systems were used together with a Hamon device comprising ten 10 Ω resistance elements for comparisons with fixed references of value 1 Ω and 100 Ω. Several other Hamon devices were used in the 1980s [25] to scale between 100 Ω and higher levels of resistance. A guarded, direct-reading resistance bridge with a double-ratio connection to eliminate lead-resistance errors was used at the 1 kΩ and 6453.2 Ω levels.

The time-dependence of the NIST ohm representation based on a bank of Thomas-type 1 Ω resistors was determined from these dc resistance comparisons with the QHE from August 1983 to May 1988. These early comparisons also provided data for the 1 January 1990 adjustment of the accepted value of the working standards, and redefinition of the NIST ohm representation, bringing close agreement between the NIST ohm representation and the international definition of the practical ohm based on the QHE [27]. The following paragraphs describe the present dc measurement chain and explain some of the auxiliary measurements that were used to estimate systematic error.

4.1 CCC bridge measurements (steps 7 and 8 in Figure 2)

In 1991, a QHR laboratory system was established specifically for maintaining the NIST ohm representation using the QHE. Also, the cryogenic current comparator (CCC) resistance scaling method [28] was developed and implemented to allow direct comparison of the QHR with stable 100 Ω wire-wound resistors. This method of dc resistance comparison makes use of the high sensitivity of superconducting quantum interference device (SQUID) magnetometry, and reduces the time required to make scaling measurements.

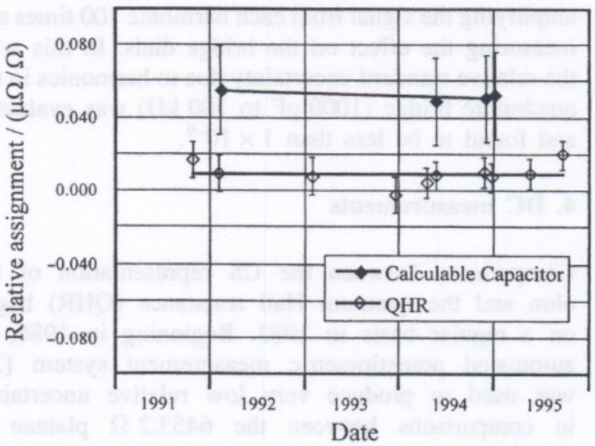

Figure 3. The two data sets plotted in Figure 3 are derived from resistance values assigned to the 1 kΩ transfer standard R311 based on the QHR representation and the calculable capacitor. The y-axis is the relative difference from $R_{K\text{-}90}$ assigned to R_K. $R_{K\text{-}90}$ would be at zero on the y-axis of this graph. Resistance R311 was used as the transfer standard in all of the comparisons from 1991 to 1995. The drift of the 1 kΩ resistor and its value determined from the QHR measurements has been removed from both sets of data. In order that only the changes in the NIST measurement values are shown, adjustment has been made to the QHR data to account for the difference between the conventional value of R_K, $R_{K\text{-}90}$, and the NIST 1988 R_K assignment from [13]. Since $R_{K\text{-}90}$ is 9×10^{-9} R_K smaller than the 1988 NIST assignment, the adjustment amounts to an increase of 0.009 μΩ/Ω for each point on the graph based on the QHR. The heavy, solid lines through the data are linear fits to the data points.

Beginning in December 1993, the QHR-based data in Figure 3 represent CCC assignments to the 1 kΩ transfer standard R311. No step-down to the 1 Ω level was required for these assignments, since the higher resistance levels were compared directly with the 100 Ω resistors. The 100 Ω resistor values were determined from the 6453.2 Ω or 12 906.4 Ω QHR plateau, and corrected for drift to assign values on the days of the comparisons with R311. The time between the measurements of the QHR and the 1 kΩ resistance typically was less than two weeks.

The 1 kΩ/100 Ω ratio was determined using a CCC constructed in 1985, together with bridge electronics built in 1991 [29]. Two other NIST CCCs were compared with this system in 1992 and 1993. The measurements used the 1 kΩ/100 Ω ratio configuration of each bridge, and were repeated over two- or three-week periods. In these comparisons, the 10 : 1 ratios agreed to within the combined relative standard uncertainty of 5×10^{-9}. The 1985 CCC was also used for 6453.2 Ω/100 Ω measurements. This ratio was compared with the 12 906.4 Ω/100 Ω ratio of another NIST CCC on at least four occasions, beginning in 1994, using a Hamon device consisting of two 6453.2 Ω resistors and either the 6453.2 Ω or the 12 906.4 Ω plateau of QHE devices. These comparisons indicate agreement between the CCC systems to within a combined relative standard uncertainty of 3×10^{-9}.

In early 1994, five stable 100 Ω standards were selected to create a 100 Ω reference bank to be used with the CCC bridges. Characterization of these resistors has shown that the average drift rate is about 5 μΩ/yr. Their temperature coefficients are quite small and only one of the five has a measurable pressure coefficient. The sets of measurements in April 1994 were the first to be based on the 100 Ω reference bank. Fifteen individual assignments were made to R311 over a period of five days in April 1994 based on 6453.2 Ω plateau QHR measurements made before and after the assignments. Each of the five 100 Ω resistors was used in three comparisons, resulting in fifteen individual measurements. The typical relative standard deviation of individual assignments using the 100 Ω reference bank was approximately 3×10^{-9}.

The November and December 1994 measurements included about fifty comparisons of the five resistors with the 6453.2 Ω and 12 906.4 Ω plateaux of two devices. In this period there was a total of thirty-four assignments to the 1 kΩ transportable standard R311. The earlier of the two sets of assignments to R311 consisted of fourteen comparisons over three days. QHR measurements were made in the following two weeks from which the mean values of the 100 Ω resistors were calculated for a mean date. Resistor R311 was then compared with the five resistors in one day of the following week, and on three consecutive days about a week later. Assignments in 1995 were made using the two plateaux and one or two QHR devices.

4.2 Comparison of QHR systems

In 1992, the NIST performed a comparison with the 1986 potentiometric system described above and a CCC measurement system using two different QHR devices in independent, closely located laboratory systems. Both QHR devices were measured at approximately 0.30 K and magnetic flux densities of about 6 T. Three 6453.2 Ω transfer resistors were compared with a heterostructure QHR device (GaAs-7) via one-to-one measurements at 25 μA using the potentiometric method. A similar QHR device (GaAs-8) was used at the 6453.2 Ω plateau with currents of 40 μA in the CCC measurements. Potentiometric assignments to the resistors were made both before and after the CCC measurements in order to close the comparison, i.e. to account for any linear drift in the resistor values. The three potentiometric assignments differed by -2×10^{-9}, -5×10^{-9}, and $+6 \times 10^{-9}$ in relative value from the CCC assignments, all with mean dates around 20 April 1992. These differences have a relative combined standard uncertainty of 8×10^{-9}.

4.3 Comparison of QHR devices

GaAs-8 and four QHR devices of the type described by Piquemal et al. [30] were compared in 1992 and 1993 at the 6453.2 Ω QHR plateau using a CCC bridge. The devices were compared in sets of two over a period of several years. Each of two devices was measured in turn against several 100 Ω wire-wound reference resistors over periods of about a week. At a relative standard uncertainty of about 4×10^{-9}, no difference between the QHR-based calibrations using the two devices was observed. In both December 1994 and May 1995, GaAs-8 and two other QHR devices were compared on both the 6453.2 Ω and 12 906.4 Ω plateaux. The 12 906.4 Ω measurements used an automated CCC system built in 1993, with source-drain currents of up to 60 μA. No differences at a relative standard uncertainty of 3×10^{-9} were detected in the QHR plateau values, nor between measurements using the different sets of Hall voltage probes of the devices.

4.4 Characterization of devices

All QHR devices were characterized using accepted techniques [31]. Characterization of the plateau longitudinal resistivity as a function of magnetic flux density B was used to determine the appropriate setting of B for the heterostructure. The plateau was verified to be flat and free of measurable dissipation over wide ranges of magnetic flux and the contact resistances were acceptably small at the measurement temperature of (0.30±0.01) K. The residual longitudinal resistivity of the devices was approximately (0.01±0.01) mΩ for the highest current levels used in NIST comparisons.

4.5 Hamon and CCC scaling comparisons

The QHR-based values assigned to resistor R311 for 1991 through early 1993 shown in Figure 3 were assigned by Hamon build-up from the 1 Ω resistor reference bank. The Hamon scaling measurements were essentially the same as in 1988. The NIST made initial scaling comparisons between CCC resistance bridges and existing Hamon devices over periods of 50 to 150 days in 1991 [28], in which both methods were used to measure a particular resistance ratio a number of times. In 1991 the average relative difference between Hamon H10A ratios and CCC bridge 100 Ω/1 Ω scaling ratios was within a relative combined standard uncertainty of 4×10^{-9}. Similar comparisons established that 1 kΩ/100 Ω and 6453.2 Ω/100 Ω Hamon ratios agreed with the CCC method. Here, the ratio differences were $+14(12) \times 10^{-9}$ and $-8(10) \times 10^{-9}$, respectively, in the initial measurements. In further comparisons in 1993 and 1994, the two methods differed by an average of $+4(10) \times 10^{-9}$ for the 1000 Ω/100 Ω ratio and $+3(10) \times 10^{-9}$ for the 6453.2 Ω/100 Ω ratio, indicating that the methods are in agreement.

4.6 Auxiliary measurements

4.6.1 Loading effects

The 1 kΩ resistor R311 was used as the transfer standard for all the comparisons linking the calculable capacitor and R_K. Both the 1989 comparison and all of the measurements of Figure 3 were carried out using this resistor at two different power levels, typically 1 mW for the QHR-based data and 4 mW for the calculable capacitor data. To determine if this resistor suffers any loading effect, another 1 kΩ resistor which has a low temperature coefficient at 25 °C was used along with transfer resistor R311 in substitution measurements. Both were measured at loads of 0.26 mW and 1.0 mW in CCC ratio measurements, and at a load of 4 mW in calculable capacitor scaling comparisons. There was about 1 μΩ difference in the comparisons between the two resistors at the three power levels, indicating that negligible loading occurs in R311 at the maximum 4 mW power level.

The CCC bridge operates with between 10 mW and 1.6 mW power dissipation in the 100 Ω resistors in ratios of 12 906.4 Ω/100 Ω, 6453.2 Ω/100 Ω, and 1 kΩ/100 Ω. Loading is not significant for the higher-valued resistors, which dissipate 1 mW or less and have low load coefficients. Comparisons of the effect of loading among different types of 100 Ω resistors [32] indicate that the NIST 100 Ω bank used in the more recent QHR measurements is free of significant loading error at power levels of up to 10 mW.

4.6.2 CCC ratio errors

Current-linkage error in a CCC system is due to incomplete superconducting shielding of the magnetic field of the CCC windings. In the NIST devices the windings are superconducting and error detection is possible using much larger currents than are used in the bridge measurements. The large current is put through sets of windings of equal turns which are connected in series-opposition. A resulting change in the magnetic flux detected by a SQUID outside the CCC would result in a systematic error in a resistance ratio. We have measured the level of current-linkage error in each CCC and found no such error at the level of 1×10^{-9}.

4.6.3 Electrical leakage

Checks for electrical leakage in the CCC bridges [33] were performed *in situ* by adding a resistance of 10 kΩ to the critical bridge link between the voltage terminals of the reference resistors. A leakage of 10^{12} Ω or less from the inner conductors to the case of the reference resistor can be detected by this method. Transfer reference R311 was found to have a leakage resistance averaging 7×10^{10} Ω at the high-potential terminals. The bridges used to measure R311 in the ac part of the calculable capacitor chain are insensitive to leakage from the resistance inner conductors to the grounded case, and a relative correction averaging 1.4×10^{-9} was thus applied to the values of resistor R311 determined using the CCC bridge. This correction takes into account the effect of the low-impedance connection to ground (the 100 Ω reference) in parallel to the leakage resistance.

4.6.4 Electronics

CCC bridge measurements are relatively insensitive to the noise level and drift of the primary bridge current. The relative drift of the primary current sources was recorded for all comparisons and contributed less than 1×10^{-9} to the relative standard uncertainty. The output of the CCC bridge is isolated by an instrumentation amplifier and optical isolator, and the gain and linearity of this circuit was measured at the end of each series of ratio comparisons. The SQUID feedback and control circuit is also optically isolated. The gains of the SQUID-based detector and conventional nanovolt amplifier need not be calibrated because both operate at null output throughout the ratio measurement by means of proportional and integral feedback.

5. Uncertainties

The uncertainties for all of our measurements are listed in Tables 1 to 3. They are shown in the form of relative standard uncertainties (i.e. one standard deviation estimates) and the last row of each table is the root-sum-square of the uncertainties above. The uncertainties listed in Tables 1 and 2 describe the ac measurements and those listed in Table 3 the dc measurements. The identifying letters refer to the second column of each table.

AC measurements

The source of the uncertainties and the method of estimation are briefly described. The uncertainties for the calculable capacitor experiment and the transfer of the value to the bank of 10 pF transfer standards are listed in Table 1 and are discussed below.

(a) Variability of repeated observations: This uncertainty is an estimate of the variability of repeated observations for the calculable capacitor experiment, which is calculated as the standard deviation of the mean of several measurements of the 10 pF capacitor with the calculable capacitor during one day's measurements.

(b) Geometrical imperfections: These estimates refer to the geometrical imperfections and effects due to interferometer alignment discussed in Section 3.

(c) Frequency corrections: This entry is the uncertainty in measuring the frequency-dependent corrections resulting from loading of the inductances of the calculable capacitor bars and the capacitance to ground in the capacitor and the bridge system.

(d) Microphonic coupling: Microphonic coupling [34] is an effect caused by the motion of trapped charge in PTFE, a material used as insulation in parts of the bridge. This effect can cause a significant error in the measurements of capacitance below 1 pF. A rough estimate of the effect is found by vibrating parts of the calculable capacitor and the bridge and measuring the effect on the bridge balance.

(e) Voltage dependence, transformer ratio measurement, bridge linearity and phase adjustment: Measurements of these quantities are discussed in earlier sections. The uncertainties are based on analysis of the techniques used to measure these effects and the corrections applied [18].

Table 1. Relative standard uncertainties (i.e. estimated relative standard deviations) in the measurement of the 10 pF bank with the calculable capacitor. The last row is the root-sum-square (rss) of the uncertainties listed in the rows above. The letters in the second column refer to Section 5, where these uncertainties are discussed in detail.

Source of uncertainty		Relative standard uncertainty
	Type A standard uncertainties	
Variability of repeated observations	(a)	2×10^{-9}
	Type B standard uncertainties	
Geometrical imperfections in the calculable capacitor	(b)	15×10^{-9}
Laser/interferometer alignment	(b)	3×10^{-9}
Frequency (loading) corrections	(c)	4×10^{-9}
Microphonic coupling	(d)	5×10^{-9}
Voltage dependence	(e)	5×10^{-9}
Transformer ratio measurement	(e)	2×10^{-9}
Bridge linearity and phase adjustment	(e)	3×10^{-9}
Detector uncertainties	(f)	2×10^{-9}
Drift between calibrations/failure to close	(g)	6×10^{-9}
Coaxial choke effectiveness	(h)	1×10^{-9}
Temperature corrections for 10 pF capacitors	(i)	2×10^{-9}
Relative standard uncertainty (rss)		19×10^{-9}

Table 2. Relative standard uncertainties (i.e. estimated relative standard deviations) in relating the 10 pF bank to the transportable 1 kΩ resistor R311. The last row is the root-sum-square (rss) of the uncertainties listed in the rows above. The letters in the second column refer to Section 5, where these uncertainties are discussed in detail.

Source of uncertainty		Relative standard uncertainty
	Type A standard uncertainties	
Variability of repeated observations	(j)	2×10^{-9}
	Type B standard uncertainties	
Voltage dependence measurements	(e)	5×10^{-9}
Transformer ratio measurements	(e)	5×10^{-9}
Bridge linearity and phase adjustment	(e)	6×10^{-9}
Detector uncertainties	(f)	3×10^{-9}
Drift between calibrations/failure to close	(g)	6×10^{-9}
Coaxial choke effectiveness	(h)	2×10^{-9}
AC/DC difference of transportable 1000 Ω resistor	(k)	5×10^{-9}
Quadrature bridge harmonics	(l)	1×10^{-9}
Auxiliary adjustments of the four-terminal-pair bridge	(m)	2×10^{-9}
Relative standard uncertainty (rss)		13×10^{-9}

Table 3. Relative standard uncertainties (i.e. estimated relative standard deviations) in relating the QHR to the transportable kΩ resistor R311. The last row is the root-sum-square (rss) of the uncertainties listed in the rows above. The letters in the second column refer to Section 5, where these uncertainties are discussed in detail.

Source of uncertainty		Relative standard uncertainty
	Type A standard uncertainties	
Variability of repeated observations in scaling QHR to 100 Ω	(n)	2×10^{-9}
Variability of repeated observations in scaling 1000 Ω to 100 Ω	(o)	2×10^{-9}
	Type B standard uncertainties	
Temperature dependence of resistors	(p)	1×10^{-9}
Loading effects of resistors	(q)	3×10^{-9}
Pressure dependence of resistors	(r)	1×10^{-9}
Leakage resistance effects	(s)	3×10^{-9}
CCC bridge	(t)	3×10^{-9}
Non-ideal QHR devices	(u)	2×10^{-9}
Drift and failure to close	(v)	3×10^{-9}
Relative standard uncertainty (rss)		7×10^{-9}

(f) Detector uncertainty: This uncertainty is an estimate of the failure of the detector system to eliminate harmonics.

(g) Drift between calibrations and failure to close: This represents an uncertainty which takes into account how well the sequence described earlier accounts for the effects of the standards drifting over time.

(h) Coaxial choke effectiveness: This entry is an estimate of the uncertainty of the coaxial choke corrections.

(i) Temperature corrections for 10 pF capacitors: Uncertainty in the temperature corrections is an evaluation of how well the temperatures of the 10 pF fused-silica capacitors can be corrected to their nominal temperatures. This is required because of the large temperature coefficients of these capacitors which cannot be neglected.

The uncertainties in relating the 10 pF bank to the 1 kΩ resistor are given in Table 2. Some are similar to those previously described and are referred to by the letters in the second column in Table 2. Only the additional uncertainties are listed below.

(j) Variability of repeated observations: The origin of this uncertainty is an estimate of the variability of the sequence of measurements (numbered 3, 4 and 5 in Figure 2) which relates the 10 pF bank to the 1 kΩ resistor R311.

(k) AC/DC difference of transportable 1000 Ω resistor: The uncertainty assigned to the ac/dc difference measurement is based on several assessments [4]: the uncertainty assigned to the calculation of the ac/dc difference of the coaxial 1000 Ω resistor discussed in Section 4; an experimental check on this calculation by comparison with a similar coaxial 100 Ω resistor at different frequencies; an estimate of dc error due to the Peltier effect assessed using an 1000 Ω quadrifilar resistor; and the uncertainty in the dc and ac measurements of the transportable 1000 Ω resistor R311.

(l) Quadrature bridge harmonics: This uncertainty results from the effect of residual quadrature bridge harmonics.

(m) Auxiliary adjustments of the four-terminal-pair bridge: This is an estimation of how well the auxiliary adjustments on the four-terminal-pair bridge work, found by introducing relatively large changes in the adjustments and then measuring the changes in the main bridge readings.

DC measurements

The main sources of uncertainty in the QHR-based calibration of the 1 kΩ resistor R311 by CCC-bridge ratio comparisons are described below and listed in Table 3.

(n) Variability of repeated observations in scaling from the QHR to 100 Ω: This uncertainty was the standard deviation calculated from direct ratio comparisons, typically made in a period of one to two weeks, between the QHR and the 100 Ω resistors. Measurements before 1993 were made using two or three 100 Ω resistors; later comparisons were made using the bank of five 100 Ω resistors described in Section 4.

(o) Variability of repeated observations in scaling from 1000 Ω to 100 Ω: This uncertainty is based on the standard deviation of repeated comparisons of R311 with the same 100 Ω resistors. Typically these observations were repeated daily over a period of three to five days.

(p) Temperature dependence of resistors: The temperature of the 100 Ω resistors and the 1 kΩ resistor R311 was measured and controlled at (25.000 ± 0.003) °C. The temperature of the two mineral-oil baths used for the two different resistance comparison steps in which R311 was measured (see Figure 1) were the same to within ± 0.003 °C. Temperature measurements were based on calibrated platinum resistance thermometers.

(q) Loading effects of resistors: Loading effects are discussed in Section 4. The evaluated uncertainty includes the effect of differences in power dissipated in the two measurements involving R311 and the two CCC ratio measurements involving 100 Ω resistors.

(r) Pressure dependence of resistors: Non-negligible pressure coefficients are observed in one of the five 100 Ω resistors used since 1993 and two of those used before 1993. The measurements were corrected for variation in the ambient pressure.

(s) Leakage resistance effects: Leakage tests revealed no significant errors except those discussed above. The combined effect of leakage was estimated and assigned a relative standard uncertainty.

(t) CCC bridge: The Type B standard uncertainty attributed to the two CCC bridge systems was evaluated from measurements of current-linkage error, primary current output, and output gain discussed in Section 4.

(u) Non-ideal QHR devices: The comparison of several QHR devices of different types, on two plateaux, and for both directions of magnetic flux, was used to determine whether any inconsistencies between devices could be observed. The uncertainty assigned is that of these comparisons.

(v) Drift and failure to close: When successive assignments to a resistor are made within a few weeks or months, the second result should be predictable from the first, to within the combined statistical uncertainties, by using the known long-term drift rate of the resistor. The differences between short-term predictions and the actual results were used to evaluate the uncertainty arising from instability in the drift rate and failure to close. This refers to how well the sequence described in Figure 2 accounts for the drift rate of the standards.

6. Results and discussion

The new assignment of an SI value for the von Klitzing constant derived from these measurements is

$$R_{\mathrm{K}} = 25\,812.8\,[1 + 0.322(24) \times 10^{-6}]\ \Omega = 25\,812.808\,31(62)\ \Omega \text{ (mean date 1994-12-26).}$$

This value was obtained through a comparison of measurements of the 1000 Ω resistor R311 derived from the calculable capacitor and from the quantum Hall experiment. The measurements are plotted in Figure 3 and the measurement values are given in Table 4. The value derived from the calculable capacitor is based on the mean of two measurements made on 1994-12-09 and 1995-01-12, resulting in a mean date of 1994-12-26. Of the measurements shown in Figure 3 only these two were used since they are the ones that were accompanied by all the necessary auxiliary measurements described in Section 3. The measurements on 1994-12-09 and 1995-01-12 are each based on the mean of two weeks of daily measurements of the sequence of measurements that relates the value of the 10 pF bank to the value of the 1 kΩ resistor R311. The value from the QHR is based on the value on 1994-12-26 from a linear regression of seven measurements between 1993-12-17 and 1995-09-25. Each of these measurements was based on the mean of measurements repeated daily over a period of three to five days. The first three QHR measurements of R311 shown in Figure 3 were obtained using Hamon scaling and not the CCC bridge. These were not used since they were not made close enough to the time of the calculable capacitor measurements.

Table 4. Measurement values for the data sets plotted in Figure 3 without removing the drift of the 1 kΩ resistor R311. The values are derived from resistance values assigned to the 1 kΩ transfer standard R311 based on the QHR representation and the calculable capacitor. Resistor R311 was used as the transfer standard in all of the comparisons from 1991 to 1995. As in Figure 3, adjustment has been made to the QHR data to account for the difference between the conventional value of R_K and the NIST 1988 R_K assignment.

Date	Assignment to R311 from calculable capacitor (μΩ/Ω)	Assignment to R311 from QHR/(μΩ/Ω)
1991-10-25		17.0010
1992-02-04		17.0340
1992-02-06	17.0804	
1993-01-29		17.1750
1993-12-17		17.2920
1994-04-20		17.3480
1994-05-26	17.4067	17.3660
1994-11-29		17.4420
1994-12-09	17.4863	
1994-12-28		17.4510
1995-01-12	17.5014	
1995-05-24		17.5106
1995-09-25		17.5703

The previous assignment in May 1988 [6] was

$$R_K = 25\,812.8\,[1 + 0.280(24) \times 10^{-6}]\ \Omega = 25\,812.807\,23(61)\ \Omega \text{ (mean date 1988-05-17).}$$

The new assignment for R_K is $4.2 \times 10^{-8} \times R_K$ larger than the value assigned in 1988. This difference has remained constant over the past three years, as illustrated in Figure 3. The two data sets plotted in Figure 3 show resistance values assigned to the 1 kΩ transfer standard R311 based on the QHR representation and the calculable capacitor. The 1 kΩ resistor R311 was used as the transfer standard in all of the comparisons from 1991 to 1995. In order that only the changes in the NIST measurement values are shown, the QHR data have been adjusted to take account of the difference between the conventional value $R_{K\text{-}90}$ and the NIST 1988 R_K assignment [13]. Since $R_{K\text{-}90}$ is $9 \times 10^{-9}\ R_K$ smaller than the 1988 NIST assignment, the adjustment amounts to an increase of 0.009 μΩ/Ω for each point on the graph based on the QHR.

Our extensive investigations of the measurement systems has resulted in two possible explanations for the difference observed between this latest assignment to R_K and the 1988 assignment.

(i) New calculations of the effects of loading in the 6453.2 Ω transfer standards [32] indicate that loading corrections for these resistors were underestimated in 1988 by approximately 4×10^{-9} Ω. This change in the loading corrections would increase the 1988 determination of R_K by $4 \times 10^{-9}\ R_K$, bringing it into slightly better agreement with the new NIST determination.

(ii) Changes in the ratio of the 100 : 1 resistance bridge current transformer are described in Section 3. We have considered the possibility that a change in the ratio such as that observed in 1994, which reversed itself later in that year, could require that earlier results be reassessed. Up to 1994, this transformer ratio had a history of being extremely stable, and it was not measured in the period just before the SI determination in May 1988. When the SI ohm determination was repeated in October 1988, the assignment of R_K was found to have increased by $2.8 \times 10^{-8}\ R_K$. This October result was not supported by all accompanying checks used with the measurement in May 1988 and was assumed to be unreliable.

There is no direct evidence that the current transformer ratio had changed from its assumed value during the series of measurements around May 1988, nor that it had returned to that value in October 1988. If this course of events had occurred, the May 1988 result would have been calculated incorrectly, and be too low by approximately $2.8 \times 10^{-8}\ R_K$. If the October 1988 measurements had been used and the correction for loading of the transfer resistors applied, the assignment of R_K would be $3.3 \times 10^{-8}\ R_K$ larger and in much better agreement with the present assignment. However, it is not possible to reach a definite understanding as to the origins of the difference between measurements which are separated by an eight-year interval.

To date, three laboratories including our own have published the results of calculable capacitor and QHE comparisons. Hartland et al. at the UK National Physical Laboratory reported a value for R_K in 1988 [35] that is higher than the result reported here by $3.4 \times 10^{-8}\ R_K$. Small et al. at the National Measurement Laboratory, Australia, in their most recent determination [36], assigned to R_K a value of 25 812.807 10(114) Ω which agrees closely with the 1988 NIST assignment, but is $4.7 \times 10^{-8}\ R_K$ lower than NIST's present value. Small's earlier reported result [37] was higher than the present NIST determination by $4.1 \times 10^{-8}\ R_K$. The difference in Small's value results from a reassessment of certain systematic corrections. The uncertainties of these assignments overlap with that of the present work.

The inverse fine-structure constant α^{-1} can be obtained from our newly measured value of R_K and (2) with no additional uncertainty. We find that $\alpha^{-1} = 137.036\,0037(33)$. Other experimental determinations of the inverse fine-structure constant α^{-1} are from a NIST low-field measurement of the proton gyromagnetic ratio in water, γ'_p(low), using a Josephson voltage standard and a QHR resistance standard [38]. They report a value of $\alpha^{-1} = 137.035\,9840(51)$ which is $14.4 \times 10^{-8}\ \alpha^{-1}$ smaller than the value reported here. Another accurate determination, by a quite different method, was reported in 1995 based on a measurement of the quotient h/m_n, (m_n is the neutron mass) using a monochromatic, polarized beam of neutrons [39]. That value is $\alpha^{-1} = 137.036\,010\,82(524)$, which is $5.2 \times 10^{-8}\ \alpha^{-1}$ larger than the present NIST value. The NIST value of α^{-1} is also in close agreement with recent quantum electrodynamic (QED) calculations of the anomalous magnetic moment of the electron a_e by Kinoshita [40], which may be combined with an accurate experimental value of a_e to derive α. This combined experimental-theoretical assignment, $\alpha^{-1} = 137.035\,999\,93(52)$ is 2.8×10^{-8} smaller than the value we report.

7. Conclusions

Periodic comparisons of the QHR with the realization of the ohm through the calculable capacitor ensure that the representation of the ohm based on the quantum Hall effect and the conventional value $R_{K\text{-}90}$ is consistent with the SI ohm. Our comparisons of the QHR and the realization of the SI ohm have been extremely consistent over the three years of measurement just completed. The results of this comparison will provide data for the least-squares adjustment of fundamental constants in 1998 or 1999. In particular, we find $R_K = 25\,812.808\,31(62)\ \Omega$ and, assuming $R_K = h/e^2$, our result implies $\alpha^{-1} = 137.036\,0037(33)$ where α^{-1} is the inverse fine-structure constant. This new assignment of the quantum Hall resistance and fine-structure constant is based on a series of measurements, whereas the 1988 value was based on a single measurement. This leads the authors to believe that the present result is more reliable and should be viewed as superseding the 1988 result. The extensive investigations which have been performed on both the ac and dc parts of this [illegible]

[illegible]

12. Taylor B. N, Witt T. J., *Metrologia*, 1989, **26**, 47-62.
13. Cage M. E., Dziuba R. F., Elmquist R. E., Field B. F., Jones G. R., Olsen P. T., Phillips W. D., Shields J. Q., Steiner R. L., Taylor B. N., Williams E. R., *IEEE Trans. Instrum. Meas.*, 1989, **38(2)**, 284-289.
14. Taylor B. N., Cohen E. R., *J. Res. Natl. Inst. Stand. Technol.*, 1990, **95(5)**, 497-523.
15. Cohen E. R., Taylor B. N., *Rev. Mod. Phys.*, 1987, **59**, 1121-1148.
16. Quinn T. J., *Metrologia*, 1989, **26**, 69-74.
17. Jeffery A., Elmquist R. E., Shields J. Q., Lee L. H., Dziuba R. F., *IEEE Trans. Instrum. Meas.*, 1997, **46(2)**, 264-268.
18. Cutkosky R. D., 1970, **74C(3), (4)**, 63-78.
19. Haddad R. J., A resistor calculable from DC to $\omega = 10^5$ rad/s, Master's Thesis, School of Engineering and Applied Science, George Washington University, Washington DC, 1969, 1-57.
20. Cutkosky R. D., Shields J. Q., *IRE Trans. Instrum.*, 1960, **I-9(2)**, 243-250.
21. Shields J. Q., *IEEE Trans. Instrum. Meas.*, 1974, **IM-23**, 345-352.
22. Jeffery A., Shields J. Q., Lee L. H., *CPEM '96 Digest*, 358-359, 17-20 June 1996.
23. Shields J. Q., *J. Res. Natl. Bur. Stand.*, 1965, **69C**, 265-274.
24. Homan D. N., *J. Res. Natl. Bur. Stand.*, 1968, **72C(2)**, 161-165.
25. Cage M. E., Dziuba R. F., Van Degrift C. T., Yu D. Y., *IEEE Trans. Instrum. Meas.*, 1989, **38(2)**, 263-269.
26. Hamon B. V., *J. Sci. Instrum.*, 1954, **31**, 450-453.
27. Belecki N., Dziuba R. F., Field B. F., Taylor B. N., Guidelines for Implementing the New Representations of the Volt and Ohm Effective January 1, 1990, *NIST Technical Note 1263*, 1989.
28. Dziuba R. F., Elmquist R. E., *IEEE Trans. Instrum. Meas.*, 1993, **42(2)**, 126-130.
29. Elmquist R. E., Dziuba R. F., *Rev. Sci. Instrum.*, 1991, **62**, 2457-2460.
30. Piquemal F., Geneves G., Delahaye F., Andre J., Patillon J., Frijlink P., *IEEE Trans. Instrum. Meas.*, 1993, **42(2)**, 264-268.
31. Delahaye F., *Metrologia*, 1989, **26**, 63-68.
32. Elmquist R. E., Dziuba R. F., *IEEE Trans. Instrum. Meas.*, 1997, **42(2)**, 126-130.
33. Elmquist R. E., *IEEE Trans. Instrum. Meas.*, 1993, **46(2)**, 322-324.
34. Shields J., *IEEE Trans. Instrum. Meas.*, 1978, **IM-27(4)**, 464-466.
35. Hartland A., Jones R. G., Kibble B., Legg D. J., *IEEE Trans. Instrum. Meas.*, 1987, **IM-36(2)**, 208-213.
36. Small G. W., Ricketts B. W., Coogan P. C., Pritchard B. J., Sovierzoski M. M. R., *Metrologia*, 1997, **34**, 241-243.
37. Small G. W., Ricketts B. W., Coogan P. C., *IEEE Trans. Instrum. Meas.*, 1989, **38(2)**, 245-248.
38. Willams E. R., Jones G. R., Ye S., Liu R., Sasaki H., Olsen P. T., Phillips W. D., Layer H. P., *IEEE Trans. Instrum. Meas.*, 1989, **38(2)**, 233-237.
39. Kruger E., Nistler W., Weirauch W., *Metrologia*, 1995, **32**, 117-128.
40. Kinoshita T., *IEEE Trans. Instrum. Meas.*, 1997, **46(2)**, 108-111.

Received on 1 October 1997.